OpenNano 7 (2022) 100057

Contents lists available at ScienceDirect

OpenNano

journal homepage: www.elsevier.com/locate/onano

Emphasized temperature dependent electrical properties study of fabricated ZnO/PVA/PANI nanocomposite films

Pratibha S Kanavi [a,*], Sunil Meti [b], R.H. Fattepur [c], Veerabhadragouda B. Patil [d]

[a] C. N. R. Rao Research Center, Basaveshwar Science College, Rani Channamma University, Bagalkot - 587101, Karantaka, India
[b] Department of Metallurgical and Materials Engineering, National Institute of Technology Karnataka, Surathkal - 575025, India
[c] Department of Physics, Raichur University, Raichur - 584101, Karnataka, India
[d] Institute of Energetic Materials, Faculty of Chemical Technology, University of Pardubice, Pardubice - 532 10, Czech Republic

ARTICLE INFO

Keywords:
Co-precipitation method
ZnO nanoflakes
Electrical conductivity
Thermal-stability
Polyniline films

ABSTRACT

Polyvinyl alcohol-Polyaniline composite films with different amounts of zinc oxide (ZnO) (0.2%, 0.4%, 0.6% and 1%)were prepared by in situ polymerization followed by film casting and drying. The samples, ZnO and PPZ films, were characterized by various techniques. The presence of ZnO in PPZ films was confirmed by the X-Ray Diffractometer (XRD). The surface morphology of the ZnO and PPZ films were examined by the Field-Emission Scanning Electron Microscopy(FESEM). The formation of absorption bonds corresponding to the PPZ films were illustrated by the Fourier Transform Infrared Spectroscope (FTIR)analysis. The films were found to be stable up to 150 °C, which was confirmed from the Differential Scanning Calorimetry (DSC) and Thermo-Gravimetric Analyzer (TGA) technique. The absorption peaks of PPZ, around visible and UV region, was studied by the UV–Vis spectra. The electrical conductivity plots obtained from the impedance analyzer, between frequency ranges of 10 Hz to 100 kHz, show that the increase in concentration and temperature of the samples resulted in the higher conductivity of the PPZ films. For 1% ZnO concentration at 150 °C, the AC conductivity of PPZ1 was found to be 20.06 S/m. Such conductivity behavior samples render the applicability of the PPZ films.

1. Introduction

Zinc oxide (ZnO) is attractive low cost semiconducting material with wide band gap (3.37 eV), which is eco-friendly [1]. It is extensively used in many applications of optical and electronic devices [2]. ZnO is used in various devices like, piezoelectric devices, gas sensors, humidity sensors, LEDs, transparent conductors, solar cells, transducers, photocatalytic materials, etc. [3]. Nano-shaped ZnO can be synthesized by various methods, but co-precipitation method has attracted much attention due to its advantages like, controlling and tuning of shape, size, morphology and growth conditions [3,4,7]. Incorporation of the ZnO nanostructures into the polymer matrix can be used to alter the conductive, mechanical, electrical properties and transparency of the films [7,9]. The addition of ZnO to the polymer matrix also improves the coefficient of friction, thermal stability and dielectric properties.

Polyaniline (PANI) is a conductive polymer obtained from the chemical polymerization of the aniline in the presence of aqueous medium of HCl and ammonium persulfate [11]. PANI is the most explored polymer due to its environmental stability and tunable

* Corresponding author at: C. N. R. Rao Research Center, Basaveshwar Science College, Rani Channamma University, Bagalkot - 587101, Karantaka, India
E-mail address: pratibharamgeri@gmail.com (P.S. Kanavi).

https://doi.org/10.1016/j.onano.2022.100057
Received 5 March 2022; Received in revised form 29 May 2022; Accepted 2 July 2022
Available online 5 July 2022

conductivity [5]. PANI polymers have the property of low solubility in aqueous medium. Addition of PVA to the PANI matrix makes it soluble in common solvents to form composites. The composites are formed by the in situ polymerization of aniline in presence of PVA [5,9]. The conductivity of PANI increases with increase in solubility and addition of surfactants. The nanostructured inorganic fillers having high surface area to volume ratio expected to modify the electrical, optical and conductive properties of polymers [5]. The nanofillers acts as smart dopants and significantly influences the properties of base polymer [12]. Due to the quantum confinement effect, the composites exhibit tremendous improvement in the properties which is the subject of current attention [13]. The hybrid inorganic/polymer composites is the currently explored area due the synergetic and complementary behavior of inorganic nanofillers and polymer material. The addition of ZnO to the PANI-PVA composites severely affects the electrical conductivity, transparency and mechanical properties of the polymer composite films [1,2,11]. The polarization decay occurs in the inorganic/polymer composites, when the frequency is applied at room temperature [10]. The phenomenon results in change in dielectric and electrical conductive properties of the PANI-PVA-ZnO (PPZ). The anomalous behavior of the PPZ composites has attracted the researchers in conduction mechanism.

The present work is mainly focused on understating the conduction mechanism and relaxation behavior of the PPZ composites. The structural, chemical, thermal and morphological studies with different weight ratios of ZnO in PPZ samples were characterized. The impedance measurements were used to analyze the electronic transportation mechanism in the prepared PPZ films under the influence of applied frequencies from room temperature to 150 °C.

2. Materials and methods

2.1. Materials

All the reagents used in the study were analytical grade and used without further purification. Zinc nitrate hexahydrate and sodium hydroxide were purchased from Sigma-Aldrich, Bangalore, India. The deionised (DI) water was used in the experiment. Here, we have used aniline hydrochloride as an aniline monomer to prepare PANI with the molecular weight 129.60 g/mol and PVA used with the viscosity 4% aqueous solution at 20 °C during the preparation of PVA/PANI/ZnO nanocomposites.

2.2. Synthesis of ZnO by co-precipitation method

A solution of 0.03 M zinc nitrate hexahydrate was prepared by dissolving in 30 ml of DI water and kept for magnetic stirring. The ratio between Zinc nitrate hexahydrate and sodium hydroxide was considered to be 1:1. About, 1.2 g sodium hydroxide was added to the solution to prepare 0.03 M of ZnO under constant stirring. A temperature of 80 °C was maintained throughout the stirring. The solution was magnetically stirred for the duration of 1 h. Further the solution was allowed to cool down to room temperature. The solution was centrifuged for five cycles at 1000 rpm for 5 min. The collected precipitate was filtered using Whatman paper and washed with ethanol [14]. The final product was annealed at 250 °C for the duration of 3 h.

2.3. PVA/PANI/ZnO film fabrication

Initially, 6.5 g of PVA was dissolved in 100 ml DI water for the duration of 1 h at 90 °C subsequently 1.3 g of aniline hydrochloride was added in to the solution after 10 min. Further, the solution was allowed to cool down to room temperature. Around 1.3 g of aniline hydrochloride was added into the above solution which was kept for magnetic stirring at 0 °C. Further, 10 ml of ammonium persulphate was added and stirred for one hour to attain the equilibrium. Finally, ZnO nanoparticles were dispersed into the solution and mechanically stirred to attain the uniformity in the solution. The whole reaction was carried out at 0 °C for 8 h [15,16]. Four different solutions containing different weight percent (0.2, 0.4, 0.6 and 1) of ZnO nanoparticles was prepared. The solutions were named as PPZ 0.2, PPZ 0.4, PPZ 0.6 and PPZ 1. The prepared solution was cast the film in a Petri dish for three days [15].

2.4. Characterization techniques

The structural properties of synthesized ZnO nanoflakes and PPZ films were characterized by X-ray diffractometry (XRD, make-Rigaku) using copper target (Cu K_α = 1.54 .Å). The morphology of synthesized ZnO nanoflakes was investigated by using field emission scanning electron microscopy (FESEM, make-ZEISS, equipped with EDS, German). The functional groups present in the film was analysed by using Fourier transform infrared (FTIR, make-PERKIN ELMER, German). The thermal properties of the PPZ films were studied by using Thermo-gravimetric analyzer (TGA, make-PERKIN ELMER, German) and Differential scanning calorimetry (DSC, NETZSCH, German). The absorption spectra were recorded by using UV–visible spectrophotometer (Systronics, Model-2201).The temperature dependent electrical conductivity is measured using the Hioki IM3536 LCR meter between 10 Hz to 100 kHz.

3. Results and discussions

3.1. XRD analysis

The XRD spectrum of as synthesized nanoparticles is identified as belonging to monoclinic cell and the C2/m space group of zinc hydroxide nitrate [$Zn_5(OH)_8(NO_3) \cdot 2H_2O$] phase (ICDD card NO. 01–072–0627) as shown in (Fig 1a. [17]. The synthesized sample

yields 100% ZnO wurzite hexagonal phase (ICDD, card No.89–0510) after annealing it at 250 °C, which is confirmed by the XRD spectrum as shown in Fig 1b.

The XRD spectra of casted PPZ films are shown in Fig 2. The peak intensities decrease with increase in ZnO concentration loading from 0.2 to 1 % in the PPZ films. The broad amorphous peak at 2Θ = 19.3° for PPZ0.2 films shows the characteristic of crystalline and amorphous phases of semi crystalline PVA in the PPZ composite film. There is a small shift in the peak towards the high angle side, when the ZnO content increases from 0.2 to 1% in the PPZ films. The intensity of the peak has also decreased after increasing of ZnO loading. This confirms that the PANI/PVA polymer chain is disrupted and distorted due to the interaction of ZnO towards the PVA/PANI chain. The crystalline peaks present at 23.5° and 35.68° are due to the regular repetition of aniline monomer in the PVA/PANI polymer chain [18]. However, the ZnO peaks are absent in the polymer composite film due to its low content. During the dispersion process, the aniline groups (-$NH3^{+}$) from the PANI are stabled to the surface of the ZnO nanoparticles [19]. The area under the curve for the peak at 19.3° also decreases which confirms the disruption in the PVA-PANI polymer chain due to the interaction with ZnO. The peak positioned around 40.5° also shifts towards higher angle side. This observation also supports that the increase in ZnO content increases the crystallinity and orderly arrangements of polymer molecular chains. It is also believed that the PVA/PANI polymer is coated over the ZnO nanoparticles [3].

3.2. SEM and EDAX analysis

The Fig 3a-d shows the scanning electron morphology of ZnO nanoflakes prepared by a simple co-precipitation method. SEM image of ZnO shows the flaky structure with a uniform distribution. The dimensions of ZnO nanoflakes are uniform throughout. The thickness of the ZnO nanoflakes varies from 20 to 50 nm as shown by the high resolution SEM image in Fig 3. The EDAX spectra of the ZnO nanoflakes confirms the presence of only zinc and oxygen (Fig 3e)

Scanning electron microscopy (SEM,) was employed to measure the surface morphology of the PPZ film. Fig 4a, represents a SEM

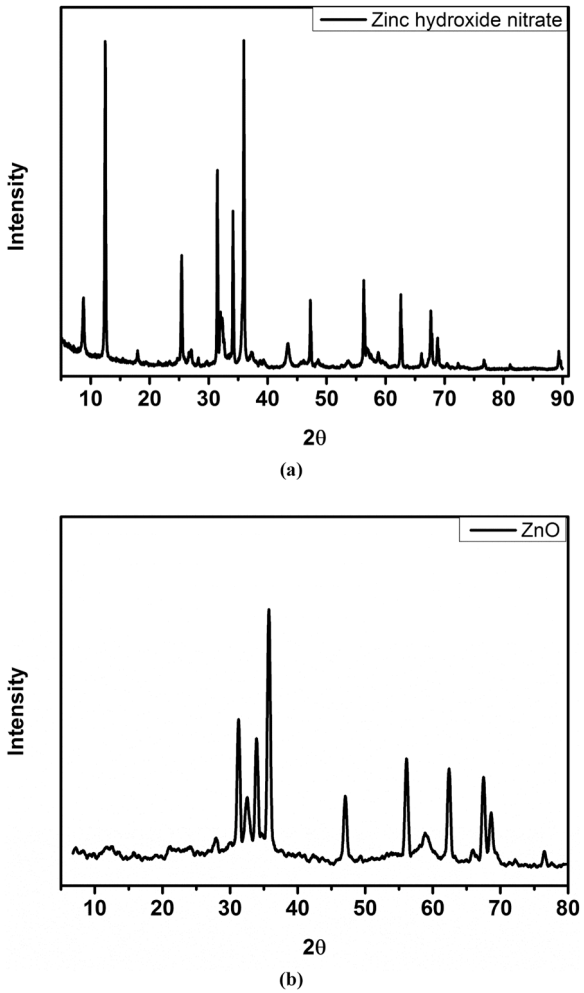

Fig 1. XRD spectra of (a) as synthesized sample and (b) sample annealed after heating at 250 °C.

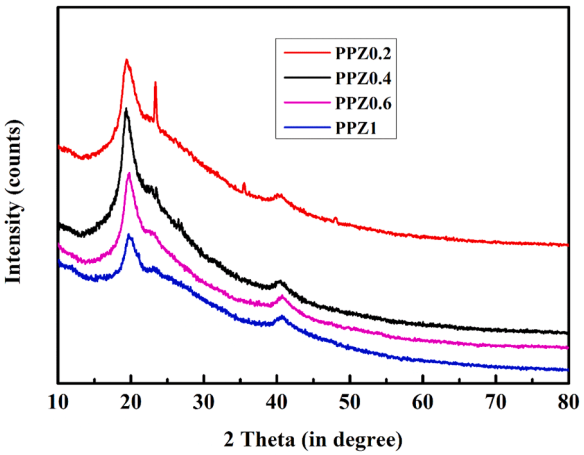

Fig 2. XRD patterns of PPZ0.2, PPZ0.4, PPZ0.6 and PPZ1 nanocomposite films.

image of PPZ film. The sensitive film exhibits micro-porous and nanofiber structures that helps to increase the charge storage reaction because the film has a large surface area. In Fig 4 we also see SEM images of the surface of the PPZ films obtained by depositing the colloidal dispersions, and after evaporation of the solvent. In Fig 4a, one can observe the formation of a homogeneous film of PANI/PVA/ZnO nanoflakes. An energy dispersive spectrometer (OXFORD INCA ENERGY 400) was used to detect elements of the PANI/PVA. Fig 4c, shows the elements of the PANI/PVA film measured by energy dispersive spectrometer. Table 1. summarizes the composition of the PANI/PVA/ZnO film. The results showed that the PPZ film contained 7.47 wt% C, 15.41 wt% N, 40 wt% O and 37.12 wt% ZnK. The C, N elements are resulted from substrate and surfactant chemicals, respectively [20]. The cross sectional image of the PPZ sample shown in Fig 4b. The thickness of the film found to be about 169 μm. The thickness was uniform throught and confirmed by the SEM images [20].

Table 2

3.3. FTIR analysis

The FTIR technique is performed to determine the functional groups and surface chemistry of the ZnO nanoflakes as shwon in Fig (5)a. The strong and broad peak detected at 3450 cm^{-1} indicates the presence of O—H stretching, which is due to the moisture in the ZnO nanoflakes. The absorption band at 1612 cm^{-1} is attributed to the strong C = C stretching peak of adsorbed carbon on the ZnO surface [21]. The sharp peak detected at 1369 cm^{-1} is corresponding to the O—H bending. Depending on the experimental conditions, the absorption peak associated with Zn-O bonds are present in the range of 800–400 cm^{-1} . The absorption peaks at 760, 632 and 424 cm^{-1} confirmed the presence of Zn-O bonds [22].

The Fig 5b, shows the FTIR spectra of the different PPZ films. The O—H, CH_2, C = O and C—O stretching characteristics peak for PVA are shown at the 3124 cm^{-1}, 2938 cm^{-1}, 1699 cm^{-1}, 1259 cm^{-1}, respectively, which are attributed to the corresponding stretching and vibration bonds [6]. The peaks present at 3221 cm^{-1} and 1408 cm^{-1} indicates the characteristics peaks of PANI in PPZ samples. The presence of ZnO nanoflakes in the PPZ samples is confirmed by the FTIR peaks observed at 475 cm^{-1} and 577 cm^{-1}.

3.4. DSC analysis

The broad endothermal peak centered around 85 °C is due to the evaporation of adsorbed water molecules on the surface of the PPZ films. The small DSC peak around 190 °C is also due to the thermal decomposition of residual zinc hydroxide nitrate into ZnO [17]. The PVA present in the PPZ composite starts melting beyond 190 °C which is shown in the DSC spectra for all the samples Fig 6. The endotherm peak at 200 °C is attributed to the cross-linking reaction between the PANI & PVA polymers in the PPZ composite films. The peak centered around 236 °C is the cross linking of ZnO nanoflakes with the PVA/PANI polymer films. The peak intensity is predominant for PPZ1 samples due to the higher content of ZnO present in the composite films [22]. The peak intensity decreases with decrease in ZnO content in the PPZ samples. The degradation of the PVA and PANI present in the PPZ samples starts at 280 °C. The degradation range increases with increase in the ZnO content in case of PPZ composite films [17]. This is due to the interaction of ZnO with polymer chains. The cross linking bonds between ZnO and polymer films becomes stronger and more predominant with increasing ZnO concentration loading in the samples.

3.5. TGA analysis

The stability of the PPZ films are tested by the Thermo-gravimetric analysis (TGA). The thermograms of the PPZ films are noted from 50 °C to 400 °C. The samples are analysed in the presence of N_2 atmosphere as shown in the Fig 7. The weight loss for the PANI

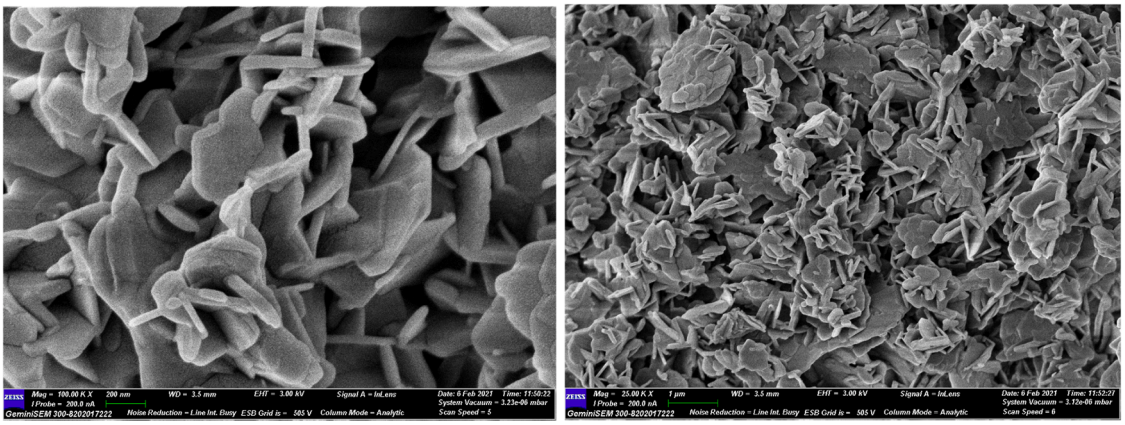

(a) (b)

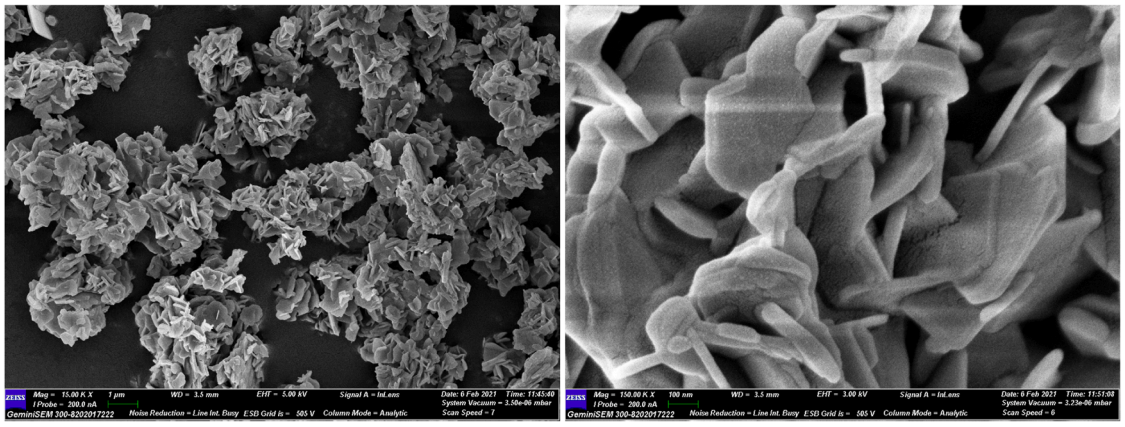

(c) (d)

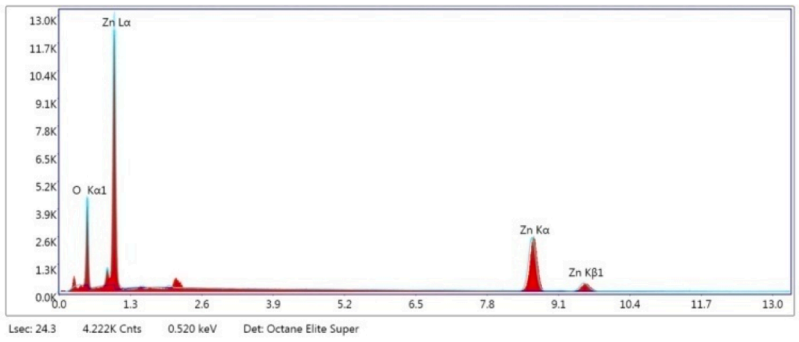

(e)

Fig 3. (a-d) FeSEM images with the magnification 100 KX, 25 KX, 15 KXand 150 KX respectively. (e) The respective EDAX spectra of ZnO nanoflakes.

polymer was containing single step degradation with overall mass loss of 18 %. The degradation of neat PANI was up to 178 °C. The weight loss for the PVA polymer was found to be gradually increasing. The overall weigh loss of the PVA polymer was calculated from the thermograms was 8.4 %. The initial weight loss at around 80 to 135 °C is due to the removal of adsorbed moisture along with a small amount of PVA in PPZ samples. The second weight loss from 135 °C upto 230 °C is ascribed to the degradation of PVA polymer. This is in good agreement with the DSC analysis. The weight loss is due to the decomposition of hydroxy groups in the PVA polymer chain [23–27]. Beyond 230 °C temperature major mass loss occuring due to the PANI polymer chain, where dehydroxylation of the co-polymer in the matrix. The total mass loss at 400 °C is almost equal to 57.24 % [28]. For comparison of TGA results with the bare

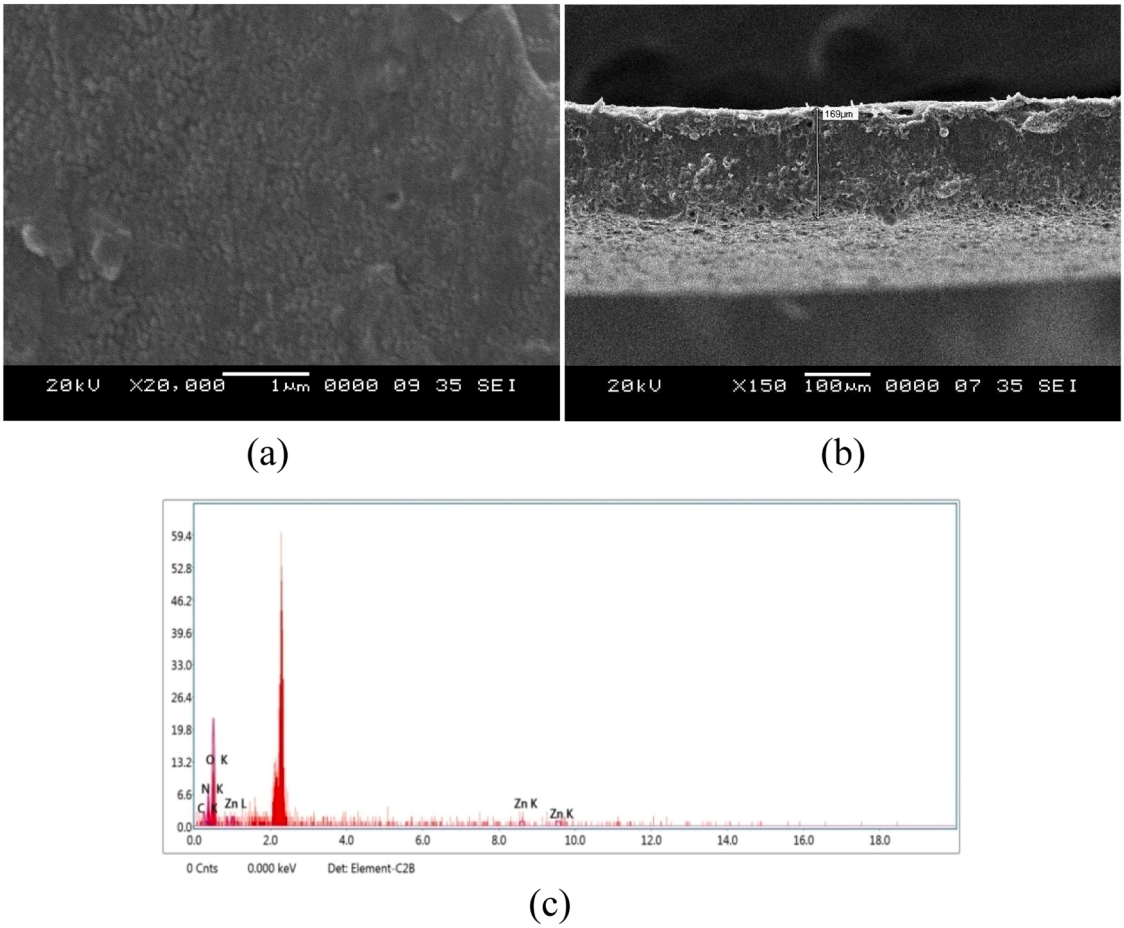

Fig 4. (a)FeSEM image of PPZ film,(b)Cross sectional image of PPZ1 film, (c)EDAX spectra of PPZ1 sample.

Table 1
Elemental composition of ZnO nanoflakes.

Element	Weight%	Atomic%	Error%
O K	12.64	37.15	6.46
ZnK	87.36	62.85	2.38

Table 2
Elemental composition of PVA/PANI/ZnO nanocomposite films.

Element	Weight%	Atomic%	Error%
C K	7.47	12.99	96.76
N K	15.41	22.97	44.01
O K	40	52.19	21.6
ZnK	37.12	11.85	20.97

matrix PVA and PANI polymer, The TGA of the polymer is recorded from room temperature to 400 °C with same conditions. The initial weight loss of 6.1 % is due to the removal of water molecules from the PVA polymer upto 130 °C. Beyond that, the weight loss of 3.1 % upto 252 °C is due to the decomposition of hydroxy groups in the PVA polymer chain. The weight loss beyond 252 °C is intense. Around 80 % of weight loss is recorded from 252 °C to 400 °C. This is due to the reason that beyond 252 °C the degradation of PVA occurs and weight loss is drastic [10] [11].

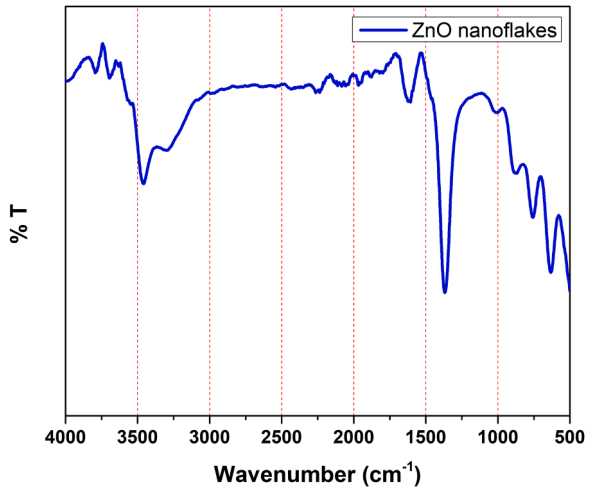

(a)

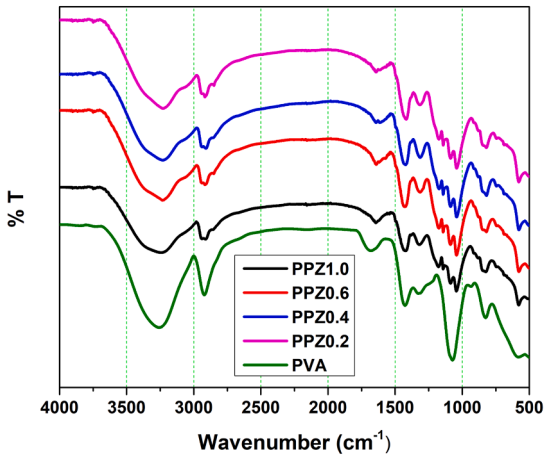

(b)

Fig 5. FTIR spectra of a) ZnO nanoflakes and b) PANI/PVA/ZnO polymer nanocomposite films having ZnO with 0.2%, 0.4%, 0.6% and 1%, respectively.

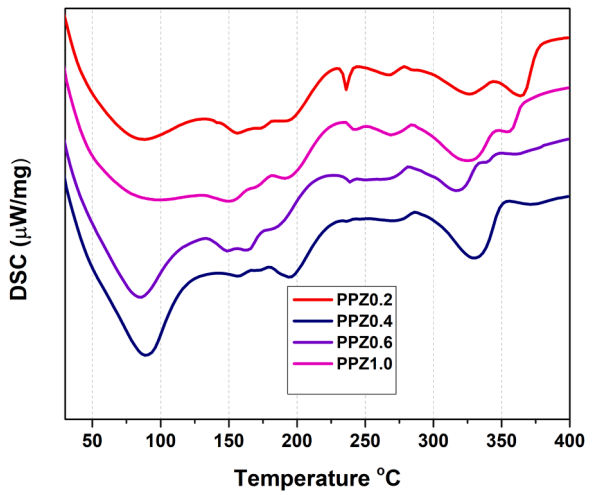

Fig 6. DSC graph of PPZ composite films.

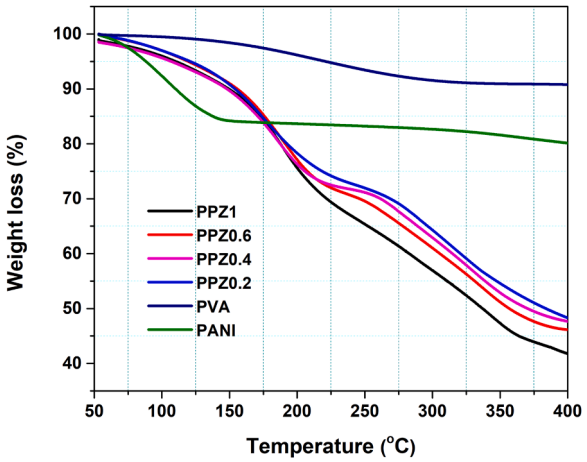

Fig 7. TGA analysis of PPZ composite films.

3.6. *UV–Visible analysis*

The UV–Visible highest absorption peak observed at 213 nm shown in Fig 8a. The peak centered at ~414 nm is the characteristic peak for hexagonal wurtzite ZnO [29]. The shifting of higher wavelength indicates the decrease of optical band gap found lower than that of 3.28 eV is represents the bulk form of ZnO, this is due to the quantum confinement effects and the presence of intrinsic crystal defects [29]. The peak at 653 nm is attributed to the presence of intrinsic crystal defects in the ZnO nanoflakes [30]. The UV–Visible

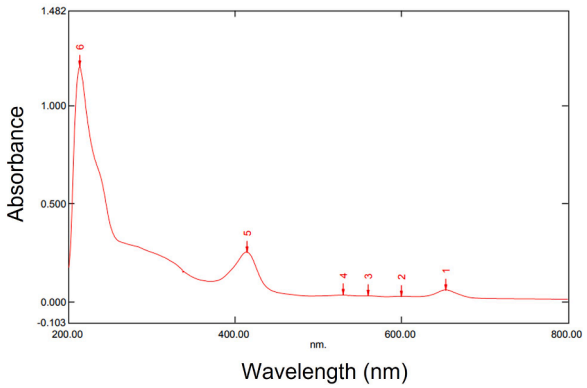

(a)

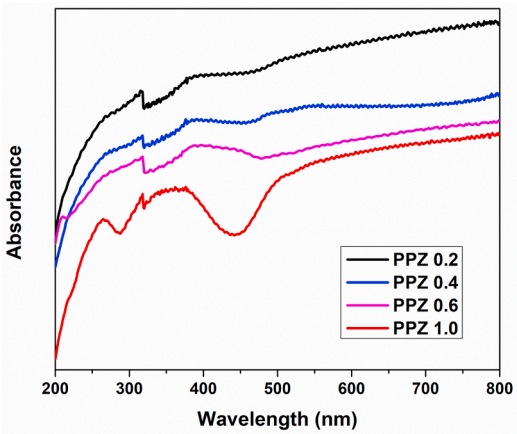

(b)

Fig 8. UV–Vis spectra of (a) ZnO nanoflakes, (b) PPZ composite films with ZnO as variable.

absorption spectra of PPZ composite films Fig 8b, are taken in the reflection mode of the sample. The UV absorption peak for characteristic nanostructured ZnO in the PPZ films is observed at 384 nm for PPZ (0.2 wt%) sample. This absorption peak shifts towards the UV region for higher loading of ZnO in the PPZ films. The energy band gap values are affected due to the Burstein-Moss effect. The absorption peaks for PPZ (0.4 wt%), PPZ (0.6 wt%) and PPZ (1 wt%) are present at 382 nm, 379 nm and 368 nm respectively. This is due to the reason of quantum confinement effect [28]. The Π-Π* transition of benzenoid (N-B-N) units of PANI is present at 322 nm. The blue shifting of absorption peak is present approximately at 520 nm. The shifting is predominantly seen for PPZ (1 wt%) film, where as it is low intense in case of other PPZ composite films [26].The blue shifting of absorption is due to the interaction of PANI-ZnO-PVA indicates the existance of ZnO for PPZ (1 wt%) sample. The existance of shoulder peak is not distinguishable for other samples or is not predominantly observed. The reason is because of lower concentration of ZnO loading.

3.7. Temperature dependent electrical conductivity of PPZ films

The temperature dependent AC conductivity spectra under the influecne of applied frequency is shown in Fig 9. At lower frequency region, the interfacial polarization occurs between the electrode and PPZ film surface as well as between the grains and interfacial region of ZnO and polymer chains. The bulk conductivity increases with increase in frequency therefore the charged species transfers easily results in increase in conductivity.The phenomenon is due to the increased kinetic energy of the conducting charges and the dipole moments [8]. The spectra shows that the conductivity increases with increase in ZnO percentage in the PVA-PANI matrix. The increase in temperature has affetected the conductivity andthe samples tend to increase its conductivity as the temperature increases from room temeprature up to 150 °C.

The conductivity mesaurements of the samples are carried out at temperature intervals of 30, 60, 90, 120 and 150 °C.All the samples PPZ0.2, PPZ0.4, PPZ0.6 and PPZ1 with respect to the different temperature intervals the conductivity versus applied frequecy (10 Hz to 100 kHz) is plotted (Fig 9a-d). The interfacial polarization with structural homogenity in the PPZ polymer nanocomposites can be identified in the low frequency region of 10 Hz to 100 kHz. A small enhancement of the conductivity is observed at room temperature for all the PPZ samples. The conductivity is less in the low frequency region between 10 Hz to 10^3 Hz. This is due to the all types of polarization, but the dipole polarization is more predominant in the region of 10^3 Hz. The electrode polrization is the main factor which affects the conductivity in this low frequency region. The dipole rotate between the two charge carriers along the axis of symmetric position [28].

The PPZ samples obeyed the universal power law, where the conductivity is independent of applied field. The power law is expressed by the following equation $\sigma(\omega) = \sigma_0 + A\omega''$, where σ_0 is the conductivity in the low frequency region and '*A*' is exponential factor. Hence, the conductivity is analoguos thouhgout the frequcny range. The changes can be observed more due to the influence of dc conductivity. It is also believed that the there is significant influence of mechanism of charge tranfer in the presence of ZnO nanofillers in the PANI-PVA matrix [16]. The Fig 10. represents the mechanism of interaction of ZnO with PVA-PANI polymer chains/matrix. When the PPZ films were subjected to increased temperature, the O^{2-} vacancies are created. The O^{2-}vacancies are corresponding to the number of uncompensated Zn^{2+}ions being generated.The number of uncompensated Zn^{2+} vacancies increases with respect to increase in oxygen content. This phenomenon results in increases in the hole concentration and enhance the higher value of electrical conductivity. It was observed from the conductivity graph that there is prominent dipole and electrode polarization in PPZ polymer nanocomposites. Among all the samples, the highest conductivity of 20.06 S/m at 100 kHz is shown by the PPZ1 sample at 150 °C (Table 3). The increased temperature, applied frequency and presence of 1 % ZnO nanofillers induces the enhanced the tarnfer of charged species within the composite. The Table 3. provides justification for the increasing in ZnO concentration in PVA/PANI matrix resulted in the increase in conductivity with respect to temperature. The samples PPZ0.2 has shown less conductivity at room temperature, which is mainly due to presence of less conductive clusters and less transfer of charged species. The σ for PPZ0.2 was found to be 2.8 S/m at 100 kHz. Conductivity of all the samples at 10^3 Hz have small variation between 0.04 S/m to 0.5 S/m for all the temeprature range. Beyond the applied frequency range of 10^3 Hz the conductivity varies from 1 S/m to 20.06 S/m.

Conclusions

The films of PVA, ZnO nanofillers and PPZ composites were successfully prepared *via* simple co-precipitation and film casting technique. The structural information of the PPZ revealed that the PANI-PVA polymers were coated over ZnO nanofillers. ZnO nanofillers were nanoflakes in nature which was helpful in binding the polymer chains to the ZnO surface. The surface morphology of the PPZ films was uniform, free of cracks and surface contamination. The cross-sectional thickness and elemental composition was also examined and shown to have no impurities. The FTIR spectra revealed that the ZnO was having chemical bonding with PVA-PANI polymer chains. Further thermal stability also realized; the PPZ films were found quite stable be loose strength and starts degrading beyond 190 °C. The AC electrical conductivity study revealed that the increase in temperature and ZnO content in polymer matrix increases the conductivity. The conductivity was found to be in the region of 0.05 to 20.06 S/m for all the samples and 1wt% found highly conductive at 150 °C This increased conductivity is attributed to the charge transfer phenomenon and interfaces formed between[1] the ZnO nanofillers and polymer chains.

[1] ZnO/PVA/PANi films, P S Kanavi et al

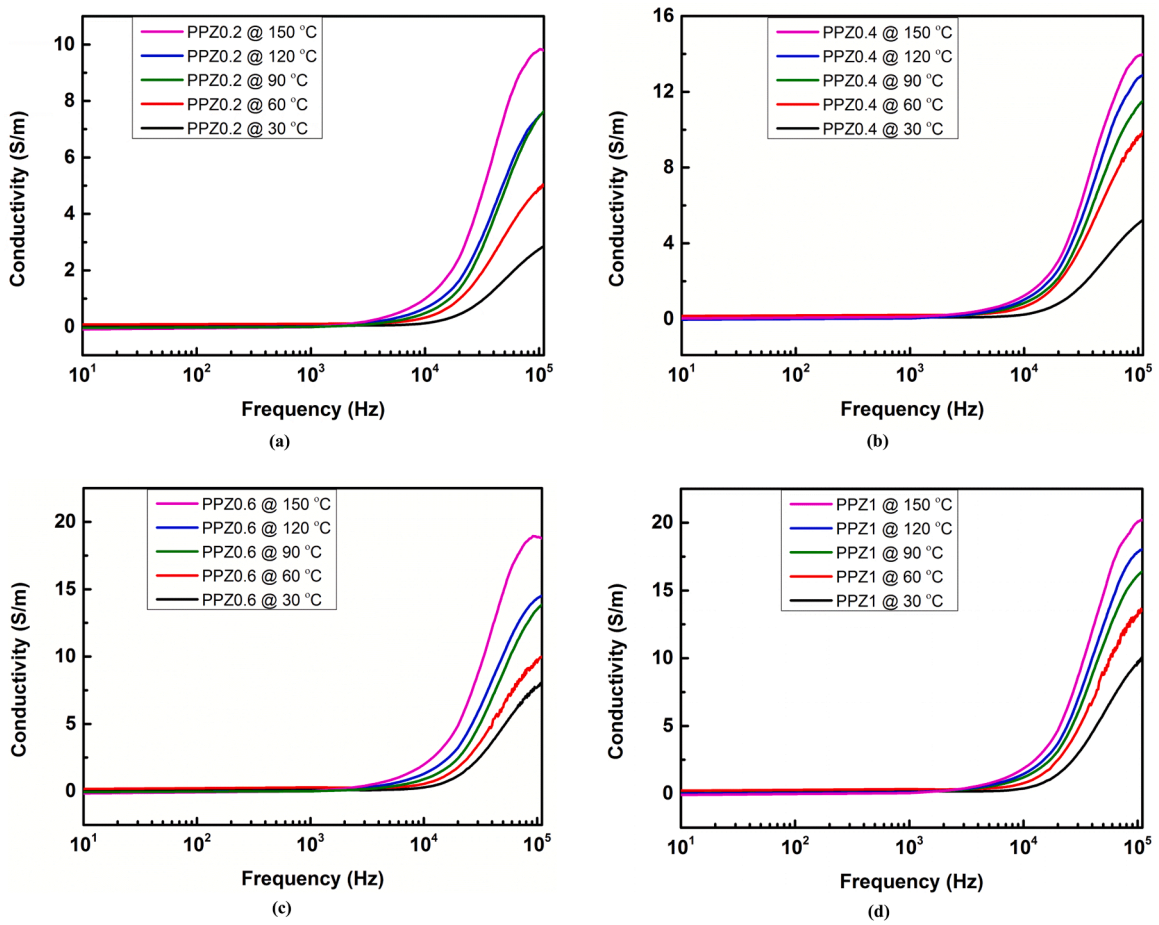

Fig. 9. Temperature dependent electrical conductivity of PPZ films, (a) PPZ0.2, (b) PPZ0.4, (c) PPZ0.6 and (d) PPZ1, against frequency.

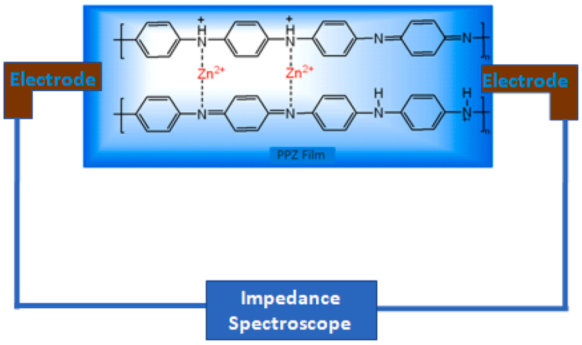

Fig 10. Schematic diagram of interaction of $Zn^{2+}$of ZnO nanoparticles with PANI polymeric chain in PVA film surface ref. [31,32].

CRediT authorship contribution statement

Pratibha S Kanavi: Conceptualization, Formal analysis, Methodology, Software, Validation, Visualization, Writing – original draft, Writing – review & editing. **Sunil Meti:** Conceptualization, Formal analysis, Methodology, Resources, Software, Validation, Visualization, Writing – review & editing. **R.H. Fattepur:** Investigation, Project administration, Supervision. **Veerabhadragouda B. Patil:** Conceptualization, Methodology, Resources, Validation, Visualization, Writing – review & editing.

Table 3
Conductivity values with different ZnO% at one particular temperature.

Sample	Temp in °C	Conductivity at 100 kHz
PVA-Pani-0.2wt% ZnO	30	2.8055
PVA-Pani-0.4wt% ZnO		5.1971
PVA-Pani-0.6wt% ZnO		8.1295
PVA-Pani-1wt% ZnO		**13.663**
PVA-Pani-0.2wt% ZnO	60	5.0579
PVA-Pani-0.4wt% ZnO		9.8935
PVA-Pani-0.6wt% ZnO		10.054
PVA-Pani-1wt% ZnO		**13.663**
PVA-Pani-0.2wt% ZnO	90	7.4825
PVA-Pani-0.4wt% ZnO		11.528
PVA-Pani-0.6wt% ZnO		13.729
PVA-Pani-1wt% ZnO		**16.431**
PVA-Pani-0.2wt% ZnO	120	7.6547
PVA-Pani-0.4wt% ZnO		12.991
PVA-Pani-0.6wt% ZnO		14.630
PVA-Pani-1wt% ZnO		**18.180**
PVA-Pani-0.2wt% ZnO	150	9.8509
PVA-Pani-0.4wt% ZnO		14.023
PVA-Pani-0.6wt% ZnO		18.964
PVA-Pani-1wt% ZnO		**20.28184**

Declaration of Competing Interest

Authors confirm that there is no conflict of interest.

Acknowledgment

Authors are grateful to B.V.V.Sangha Basaveshwar Science College, Bagalkot for providing facility to perform experiments. Author PSK are thankful to DST-SAIF, Scientific instrumentation Center, Karnataka University, Dharwad for their help during XRD, SEM and EDAX analysis. Authors would like to thankSECAB Institute, Vijayapur, providing facility for spectral analysis.

References

[1] Ü. Özgür, Y.I. Alivov, C. Liu, A. Teke, M.A. Reshchikov, S. Doğan, V. Avrutin, S.J. Cho, H. Morkç, A comprehensive review of ZnO materials and devices, J. Appl. Phys. 98 (2005) 1–103, https://doi.org/10.1063/1.1992666.
[2] H. Singh, D. Kumar, K.K. Sawant, N. Devunuri, S. Banerjee, Co-doped ZnO–PVA nanocomposite for EMI shielding, Polym. - Plast. Technol. Eng. 55 (2016) 149–157, https://doi.org/10.1080/03602559.2015.1070869.
[3] Q. Li, V. Kumar, Y. Li, H. Zhang, T.J. Marks, R.P.H. Chang, Fabrication of ZnO nanorods and nanotubes in aqueous solutions, Chem. Mater. 17 (2005) 1001–1006, https://doi.org/10.1021/cm048144q.
[4] S. Meti, M.R. Rahman, M.I. Ahmad, K.U. Bhat, Chemical free synthesis of graphene oxide in the preparation of reduced graphene oxide-zinc oxide nanocomposite with improved photocatalytic properties, Appl. Surf. Sci. 451 (2018) 67–75, https://doi.org/10.1016/j.apsusc.2018.04.138.
[5] B.K. Sharma, A.K. Gupta, N. Khare, S.K. Dhawan, H.C. Gupta, Synthesis and characterization of polyaniline-ZnO composite and its dielectric behavior, Synth. Met. 159 (2009) 391–395, https://doi.org/10.1016/j.synthmet.2008.10.010.
[6] J. Wang, H. Chi, A. Zhou, R. Zheng, H. Bai, T. Zhang, Facile synthesis of multi-functional elastic polyaniline/polyvinyl alcohol composite gels by a solution assembly method, RSC Adv 10 (2020) 22019–22026, https://doi.org/10.1039/d0ra02238a.
[7] S. Choudhary, R.J. Sengwa, ZnO nanoparticles dispersed PVA–PVP blend matrix based high performance flexible nanodielectrics for multifunctional microelectronic devices, Curr. Appl. Phys. 18 (2018) 1041–1058, https://doi.org/10.1016/j.cap.2018.05.023.
[8] A.S. Roy, S. Gupta, S. Sindhu, A. Parveen, P.C. Ramamurthy, Composites : part B Dielectric properties of novel PVA /ZnO hybrid nanocomposite films, Compos. Part B. 47 (2013) 314–319, https://doi.org/10.1016/j.compositesb.2012.10.029.
[9] R.M. Mohsen, S.M.M. Morsi, M.M. Selim, A.M. Ghoneim, H.M. El-Sherif, Electrical, thermal, morphological, and antibacterial studies of synthesized polyaniline/zinc oxide nanocomposites, Polym. Bull. (2019) 76, https://doi.org/10.1007/s00289-018-2348-4.
[10] M.C. Arenas, G. Sánchez, O. Martínez-álvarez, V.M. Castaño, Composites : part B Electrical and morphological properties of polyaniline – polyvinyl alcohol in situ nanocomposites, Compos. Part B. 56 (2014) 857–861, https://doi.org/10.1016/j.compositesb.2013.09.010.
[11] D. Ponnamma, Q. Guo, I. Krupa, M.A.S.A. Al-Maadeed, K.T. Varughese, S. Thomas, K.K. Sadasivuni, Graphene and graphitic derivative filled polymer composites as potential sensors, Phys. Chem. Chem. Phys. 17 (2015) 3954–3981, https://doi.org/10.1039/c4cp04418e.
[12] D. Ponnamma, J. Cabibihan, M. Rajan, S.S. Pethaiah, K. Deshmukh, J. Prasad, S.K.K. Pasha, M.B. Ahamed, J. Krishnegowda, B.N. Chandrashekar, A. Reddy, C. Cheng, Materials Science & Engineering C Synthesis, optimization and applications of ZnO /polymer nanocomposites, Mater. Sci. Eng C. 98 (2019) 1210–1240, https://doi.org/10.1016/j.msec.2019.01.081.
[13] V. Koutu, P. Ojhab, L. Shastri, M.M. Malik, Study of the effect of temperature gradient on the thermal and electrical properties of ZnO nanoparticles, AIP Conf. Proc. (2018) 1953, https://doi.org/10.1063/1.5032613.
[14] H. SM, Optical properties for prepared polyvinyl alcohol/polyaniline/ ZnO nanocomposites, Iraqi J. Phys. 16 (2018) 181–189, https://doi.org/10.30723/ijp.v16i36.42.
[15] A. Samzadeh-Kermani, M. Mirzaee, M. Ghaffari-Moghaddam, Polyvinyl alcohol/polyaniline/ZnO nanocomposite: synthesis, characterization and bactericidal property, Adv. Biol. Chem. 6 (2016) 1–11, https://doi.org/10.4236/abc.2016.61001.
[16] C.V. Ruiz, E. Rodríguez-Castellón, O. Giraldo, Structural analysis and conduction mechanisms in polycrystalline zinc hydroxide nitrate, Inorg. Chem. 57 (2018) 9067–9078, https://doi.org/10.1021/acs.inorgchem.8b01074.
[17] O. Norfazlinayati, Z.A. Talib, N.G. Nik Salleh, A.H. Shaari, H. Mohd Hamzah, Synthesis and characterization of polyvinyl alcohol /polyaniline/functionalized multiwalled carbon nanotube composite by gamma radiation method, Int. J. Nanoelectron. Mater. 11 (2018) 435–448.

[18] K. Rathidevi, N. Velmani, D. Tamilselvi, Electrical conductivity study of poly (p -anisidine) doped and undoped ZnO nanocomposite, 9 (2019) 403–410.
[19] T. Khalafi, F. Buazar, K. Ghanemi, Phycosynthesis and enhanced photocatalytic activity of zinc oxide nanoparticles toward organosulfur pollutants, Sci. Rep. 9 (2019) 1–10, https://doi.org/10.1038/s41598-019-43368-3.
[20] M. Alam, N.M. Alandis, A.A. Ansari, M.R. Shaik, Optical and electrical studies of polyaniline/ZnO nanocomposite, J. Nanomater. (2013) 1–5, https://doi.org/10.1155/2013/157810, 2013.
[21] J.M. Guerrero, A. Carrillo, M.L. Mota, R.C. Ambrosio, F.S. Aguirre, J. Ding, Y. Li, M. Li, molecules purification and glutaraldehyde activation study on HCl-doped PVA-PANI copolymers with different aniline concentrations, Molecules (2019). https://doi.org/10.3390/molecules24010063.
[22] H.S. Mansur, C.M. Sadahira, A.N. Souza, A.A.P. Mansur, FTIR spectroscopy characterization of poly (vinyl alcohol) hydrogel with different hydrolysis degree and chemically crosslinked with glutaraldehyde, Mater. Sci. Eng. C. 28 (2008) 539–548, https://doi.org/10.1016/j.msec.2007.10.088.
[23] R. Ullah, Ternary composites of polyaniline with polyvinyl alcohol and Cu by inverse emulsion polymerization : a comparative study, Adv. Polym. Technol. (2018) 3448–3459, https://doi.org/10.1002/adv.22129.
[24] P.M. Visakh, Polyaniline-Based Blends, Composites, and Nanocomposites, Elsevier Inc, 2018, https://doi.org/10.1016/b978-0-12-809551-5.00001-1.
[25] S. Morimune, T. Nishino, T. Goto, Poly(vinyl alcohol)/graphene oxide nanocomposites prepared by a simple eco-process, Polym. J. 44 (2012) 1056–1063, https://doi.org/10.1038/pj.2012.58.
[26] F. Reguieg, L. Ricci, N. Bouyacoub, M. Belbachir, M. Bertoldo, Thermal characterization by DSC and TGA analyses of PVA hydrogels with organic and sodium MMT, Polym. Bull. 77 (2020) 929–948, https://doi.org/10.1007/s00289-019-02782-3.
[27] A.J. Wooten, D.J. Werder, D.J. Williams, J.L. Casson, J.A. Hollingsworth, Solution - liquid - solid growth of ternary Cu - In - Se semiconductor nanowires from multiple- and single-source precursors, J. Am. Chem. Soc. (2009) 16177–16188, https://doi.org/10.1021/ja905730n.
[28] C.J.G. Krishnaiah, K.S.A. Divya, Effect of dysprosium dopant on EPR, magnetic and electrical properties of ZnO nanoparticles, J. Mater. Sci. Mater. Electron. 29 (2018) 18159–18166, https://doi.org/10.1007/s10854-018-9928-9.
[29] M. Pudukudy, Manoj Pudukudy, Zahira Yaakob, Facile synthesis of Quasi spherical ZnO nanoparticles with excellent photocatalytic activity, J.Clust.Sci 26 (4) (2014) 1187–1201, https://doi.org/10.1007/s10876-014-0806-1.
[30] A.M. Mostafa, Preparation and study of nonlinear response of embedding ZnO nanoparticles in PVA thin film by pulsed laser ablation, J. Mol. Struct. 1223 (2021), 129007, https://doi.org/10.1016/j.molstruc.2020.129007.
[31] “Turn-off fluorescent sensing of energetic materials using protonic acid doped polyaniline: A spectrochemical mechanistic approach” Veerabhadragouda B Patil, Satish A Ture, Channabasaveshwar V Yelamaggad, Mallikarjuna N Nadagouda, Abbaraju Venkataraman; Zeitschrift für anorganische und allgemeine Chemie; doi:10.1002/zaac.202000321.
[32] Detection of energetic materials via polyaniline and its different modified forms, Veerabhadragouda B Patil, Mallikarjuna N Nadagouda, Satish A Ture, Channabasaveshwar V Yelamaggad, Abbaraju Venkataraman; Polymers for advanced Technologies Wiley; doi:10.1002/PAT.5458.